Carbohydrate Polymers 104 (2014) 135–142

Contents lists available at ScienceDirect

Carbohydrate Polymers

journal homepage: www.elsevier.com/locate/carbpol

Functionalized celluloses and their nanoparticles: Morphology, thermal properties, and solubility studies

Priyanka R. Sharma, A.J. Varma*

Polymer Science & Engineering Division, CSIR-National Chemical Laboratory, Pune 411008, India

ARTICLE INFO

Article history:
Received 3 December 2013
Received in revised form 4 January 2014
Accepted 4 January 2014
Available online 20 January 2014

Keywords:
Cellulose
6-Carboxycellulose
Nanoparticles
DTG
TGA
Morphology

ABSTRACT

Agricultural residues derived cellulose was used to synthesize a new series of carboxy functionalized cellulosic nanoparticles (quasi-spherical shaped, 13.2–21.5% carboxyl content) and macro-sized 6-carboxycelluloses (long-fibril shaped, 1.7–22% carboxyl content). The DP (50–70) and yield (upto 46%) of nanoparticles were manipulated by controlling the reaction temperature and time. TGA/DTG thermographs of the carboxycelluloses gave thermostability data and co-related well with the residual crystalline, amorphous, and anhydroglucuronic acid content. The particle shape and size had no effect on the thermal stability. Some derivatives were fully or partially soluble in aqueous alkali and non-aqueous solvents, which can lead to increased versatility of these polymers.

1. Introduction

In recent years, deforestation concerns have led to the development of non-wood sources of cellulose, especially cellulose extracted from agricultural wastes such as sugarcane bagasse, wheat straw, rice straw, etc. (Nuruddin et al., 2011; Varma, 2013). This source of cellulose is considered environment-friendly, as fewer forest trees have to be cut to produce cellulose. Another major advancement in the field of cellulose chemistry and technology is the development of nanoparticles of cellulose and cellulose derivatives (Eichhorn, 2011; Kulterer et al., 2012; Nikolajaski, Wotschadlo, Clement, & Heinze, 2012). Since most of these cellulose and nanocellulose molecules are biocompatible and biodegradable, their role in several biomedical applications, biosensors, diagnostic molecular probes, drug delivery vehicles, etc. are being vigorously pursued, along with other exciting applications in biocomposites, membranes, electronics, and solar cells (Klemm, Heublin, Fink, & Bohn, 2005; Klemm et al., 2011; Lin, Huang, & Dufresne, 2012; Zhou et al., 2013). As in metal nanoparticles, research on nanocelluloses has expanded to include shape-selective synthesis, such as nanofibres and nanospheres (Isogai, Saito, & Fukuzumi, 2011; Kulterer et al., 2012; Nikolajaski et al., 2012; Sharma & Varma, 2013). Graphene–cellulose paper membranes have been used as electrodes for flexible super capacitors. Celluloses have also been used with carbon nanotubes and combined with conducting polymers for the fabrication of electroconductive composites; further, hybrid inorganic–organic nanocomposites are emerging as a new class of functional nanomaterials (Lin et al., 2012; Shi, Philpis, & Yang, 2013). 6-Carboxycelluloses, prepared by oxidation of cellulose, have been extensively investigated for over seventy years due to their applications in wound dressing gauzes and several other related biomedical applications (Anderson & McIntyre, 1946; Houser, 1946; Kennedy, 1947; Scarff, Stookey, & Garcia, 1949). The earliest report on oxidation of cellulose to produce carboxylated cellulose was reported way back in 1883 (Cross & Bevau, 1883). Since then there have been regular streams of papers and patents on various methods of oxidation of cellulose and their applications (Kumar & Yang, 2002; Nooy, Pagliaro, Bekkum, & Besemer, 1997; Okita, Saito, & Isogai, 2010; Shinoda, Saito, Okita, & Isogai, 2012; Yackel & Kenyon, 1942). In recent years, nanofibres of 6-carboxycelluloses have also been synthesized and their properties have been investigated (Crawford et al., 2012; Nachtkamp et al., 2012; Okita et al., 2010; Shinoda et al., 2012). Indeed, carboxy functionalized nanocelluloses can be expected to vastly expand the range of properties of electroconductive devices and biomedical devices, where currently un-functionalized nanocelluloses are used. This was the motivation for taking up the synthesis and characterization of both macro-sized carboxycelluloses and nano-sized carboxycelluloses, and to compare their thermal properties, morphological changes in the products, and solubility characteristics. These are all key properties for fabricating new devices based on these materials.

* Corresponding author. Tel.: +91 20 25902178; fax: +91 20 25902618.
E-mail addresses: aj.varma@ncl.res.in, aj.varma@yahoo.com (A.J. Varma).

0144-8617/$ – see front matter © 2014 Elsevier Ltd. All rights reserved.
http://dx.doi.org/10.1016/j.carbpol.2014.01.015

Table 1
(A) Percent carboxyl content, yield and DP (degree of polymerization) of 6-carboxycelluloses at different temperatures and time periods (*NP: nanoparticles). (B) Solubility of various carboxyl content 6-carboxycelluloses (6CC) in aqueous alkali solutions. (C) Solubility of various carboxyl content 6-carboxycelluloses (6CC) in organic solvents (the part of the data of (A) showing carboxyl group contents is taken from the Supplementary Data File of our earlier published paper, Sharma & Varma, 2013).

(A)

Time (h)	—COOH content (%)*				Yield (%)/DP			
	25 °C	40 °C	50 °C	70 °C	25 °C	40 °C	50 °C	70 °C
1	1.7	6.17	–	–	84.0/87	83.0/86	–	–
3	3.0	13.2	–	–	73.0/86	72.0	–	–
6	8.6	14.3	–	–	71.0/84	68.0/81	–	–
8	–	–	–	13.9	–	–	–	16.0*/50
12	14.1	14.0	13.2	–	69.0/82	60.0/78	46.0*/70	–
24							–	–
(I crop)	19.7	16.0	–		63.0/79	25.0/77		
(II crop)*		18.0				5.0*/70		
48							–	–
(I crop)	22.0	17.0	–	–	45.0/77	22.0/76		
(II crop)*		21.5				5.0*/70		

(B)

NaOH (%)	22%6CC	14%6CC	8%6CC	3%6CC
10	++	++	++	±
5	++	++	++	−−
2	++	++	++	−−
0.4	++	++	+	−−
0.2	++	+	−−	−−

(C)

Solvents(1% solution)	22%6CC
CH_3CN	−−
DMAc	−−
DMSO	±
Dioxane	−−
Acetone	−−
Methanol	−−
Ethanol	−−
$CHCl_3$	−−
DCM	−−
THF	−−
Toluene	−−
DMF	−−
Pyridine	−−

We recently patented our work based on extraction of cellulose from non-wood sugarcane bagasse (Varma, 2013). This cellulose was oxidized to 6-carboxycellulose, and the synthesis was fine-tuned so as to produce the usual macro-sized fibrils in addition to quasi-spherical shaped nanoparticles of narrow polydispersity, narrow size range (25–35 nm), and low degrees of polymerization (Sharma & Varma, 2013). We studied the solubility characteristics of this new series of 6-carboxycelluloses (1.7–22% carboxyl content) and their nanoparticles, and also made a comparative study of the thermal properties of the materials. These results were used for deciphering gradual changes in the morphology of the cellulosic molecules caused during progressive carboxylation. Several properties of semi-crystalline polymeric molecules are guided by their morphology, thermal properties and solubilities. Hence it is important to have a good knowledge of the thermal properties and morphology as a function of degree of carboxy substitution, molecular weights, molecular sizes, and molecular shapes of the different 6-carboxycelluloses. Our previous work on aldehyde, carboxy, and amine functionalized wood cellulose as reinforcements in epoxy composites had shown interesting advantages as compared to the use of un-functionalized cellulose (Varma & Chavan, 1994). Commercial availability of nano-carboxycellulose will most certainly lead to the development nano-biocomposites of such materials. Therefore we believe our current studies throw useful new light on the utilization of forest-free cellulose for preparing carboxy functionalized celluloses and their nanoparticles for developing their applications.

2. Experimental

2.1. Synthesis of 6-carboxycellulose in non-nano and quasi-spherical nanoparticle forms

The methodology to prepare quasi-spherical shaped nanoparticles was recently published (Sharma & Varma, 2013). We could also obtain non-nano sized fibrils by this method. In general, to finely powdered sugarcane bagasse cellulose (10 g) was added 140 ml acid mixture (2:1 ratio, v/v) of 65% HNO_3 and 85% H_3PO_4 over a period of 5 min. The acid mixture was allowed to get absorbed in the cellulose for 10–15 min. This was followed by slowly adding 1.96 g of $NaNO_2$ (1.4%, w/v). As soon as the $NaNO_2$ was added, reddish fumes of NO_2 gas were evolved. The reaction was performed at three different temperatures: 25 °C, 40 °C, 50 °C and 70 °C, as shown in Table 1. The reaction mixture was quenched by diluting with distilled water (5 times the volume of acid mixture), allowed to settle down for 30 min, then decanted off. The solid part was washed with water (3 times) then with water–methanol mixture (2:1, v/v), then centrifuged at 2000 rpm to remove the solid.

The reaction products at 25 °C were obtained as single crops, none of which had the form of nanoparticles. In the specific case of the reaction at 40 °C (24 h and 48 h), after centrifugation of the initial solid at 2000 rpm for 15 min, the supernatant liquid was cloudy. This cloudy supernatant liquid was separately centrifuged at 12,000 rpm for 15 min which resulted in the separation of a second crop. The latter on analysis showed it to be

quasi-spherical shaped nanoparticles of narrow size distribution (25–35 nm).

For the reactions at 50 °C (12 h) and 70 °C (8 h) centrifugation had also to be carried out at 12,000 rpm for 15 min to allow the nanoparticles to settle down and be collected. In both these cases the entire product consisted of nanoparticles in a single crop.

2.2. Preparation of amorphous cellulose

Sugarcane bagasse based cellulose I (1 g) was taken with o-phosphoric acid (85%) (5 ml) and stirred continuously for 14 h at 25 °C, and then further stirred at 50 °C for 2 h. The cellulose was completely dissolved in the acid and was re-precipitated by slowly pouring into distilled water under stirring. The washing was done initially with water, then with methanol/water (2:1, v/v), to obtain amorphous cellulose (Wei, Kumar, & Banker, 1996).

2.3. Degree of polymerization (DP)

The degree of polymerization of the oxidized celluloses were estimated by measuring the viscosity (cP) according to standard method TAPPI T 254 cm-10. The viscosity (cP) obtained for various oxidized celluloses were used to calculate the degree of polymerization using the graphical data taken from pg.99 of the standard book "Wood and Cellulose Science" by A.J. Stamm (Stamm, 1964). We were able to tailor the DP by controlling the reaction temperature. At 40 °C and 50 °C we obtained a DP of 70, while at 70 °C we obtained a DP of 50.

2.4. Determination of carboxyl content

The carboxyl content of oxidized cellulose was measured according to the method described by United State Pharmacopeia (USP, 1995). A 0.5 g of sample was taken and emerged in 50 ml of 2% calcium acetate solution for 30 min. The mixture is then titrated with 0.1 N NaOH (standardized) by using phenolphthalein as an indicator. The volume of NaOH used was corrected by blank titration. The % carboxyl content in sample was calculated by following formula:

$$\text{Carboxyl content}\quad (\%) = \frac{N \times V \times \text{MW}\quad (\text{COOH})}{\text{Wt.}\quad \text{of sample}\quad (\text{mg})} = \times 100$$

where N is the normality of NaOH and V is the volume of NaOH used in titration.

2.5. Thermogravimetry (TGA) and differential thermogravimetry (DTG)

The thermal stability of partially oxidized cellulose was studied using Perkin Elmer STA-6000 (Simultaneous Thermal Analyzer) instrument. The samples were run at a heating rate of 10 °C/min in the range 30–850 °C, under nitrogen atmosphere.

2.6. Fourier transform infrared spectrometry (FTIR)

A Perkin Elmer Spectrum One instrument was used to record FTIR in transmission mode, between 450 and 4000 cm^{-1}. A total of 6 scans were taken per sample with a resolution of 4 cm^{-1}. The samples were recorded by using the KBr pellets prepared by using finely grinded samples (3 mg) mixed with dry KBr powder (150 mg) (the spectra are presented in the Electronic Supplementary Data file).

2.7. Scanning electron microscopy (SEM)

The scanning electron micrograph (SEM) was obtained using dual beam scanning electron microscope (FEI company, model Quanta 200 3D) operating at 30 kV. The samples were loaded on stubs and sputtered with thin gold film to prevent surface charging and also to protect them from thermal damage due to electron beam.

2.8. Transmission electron microscopy (TEM)

Transmission electron microscopy (TEM) studies of 6-carboxycellulose nanoparticles were carried out by using FEI-Technai G^2-20 instrument. A 10 μL aliquot sample of 1 mg of 6-carboxycellulose in 10 ml distilled water was mounted on freshly glow discharged carbon coated Cu grids (200 mesh, ICON Analytical, India). TEM was observed without staining the samples.

3. Results and discussions

Cellulosic nanoparticles have long defied production on a large scale, which has affected their large scale industrial use. While 6-carboxy functionalized celluloses have successfully proven their utilization in medical products such as wound gauzes and haemostatic material, most of the products have been based on the use of regenerated cellulose, i.e., cellulose II. The great disadvantage of cellulose II is that it requires severe chemicals and energy inputs for conversion from cellulose I (Cheng et al., 2011; Fink, Weigel, Purz, & Ganster, 2001; Sasaki, Adschiri, & Arai, 2003).

This paper has attempted to prepare 6-carboxycellulose from waste agricultural non-wood sources of cellulose I, avoiding the use of forest-wood which can cause environmental damage due to depletion of forest cover. Further, availability of nanoparticles of 6-carboxycelluloses could result in improved performance of the currently used macro-sized 6-carboxycelluloses in certain high-technology applications, especially biomedical applications (Varma & Sharma, 2013). Most syntheses of 6-carboxycelluloses are based on the reaction of nitrosonium ion (NO^+) with cellulose in a heterogenous reaction medium. Dinitrogen tetraoxide gas in carbon tetrachloride, TEMPO with sodium bromide/sodium chlorite, and sodium nitrite in nitric acid/phosphoric acid media have been the most investigated methodologies for the synthesis of 6-carboxycelluloses. Synthesis of 6-carboxycelluloses using dinitrogen tetraoxide gas requires high pressure (70 atm), oxidation reaction is slow and produces many by-products (Coseri et al., 2013; Zimnitski, Yurkshtovich, & Bychkovsky, 2004). Other oxidation systems based on TEMPO/NaBr/NaClO are of more recent origin, and produce long fibrils (Isogai & Kato, 1998; Okita et al., 2010). In this work we adapted the nitric acid/phosphoric acid solvent system to produce a range of 6-carboxycelluloses, including nanoparticles of quasi-spherical shapes, narrow size dispersion (25–35 nm) and low degrees of polymerization (DP 50–70). The strongly acidic medium is known to be highly temperature sensitive and causes loss of molecular weight. Hence most reports have limited the temperature range from 20 to 25 °C (Arendt, Carriere, Bouchez, & Sachetto, 1973; Kumar & Yang, 2002). However, in our experience, we found that up to 40 °C, the yields were comparable to that obtained at 25 °C for reaction times up to 12 h (Table 1). As expected, the kinetics of the reaction are highly dependent on the temperature. The initial rates of oxidation reaction were much higher at 40 °C, for e.g. a of 13.2% was achieved after 3 h reaction time, as compared to 3.0% carboxyl content for the 25 °C reaction temperature. At 12 h reaction time, the carboxyl content was about the same for the reactions at 25 °C and 40 °C. Thereafter, the yields as well as differential rates of carboxylation decreased, and only a

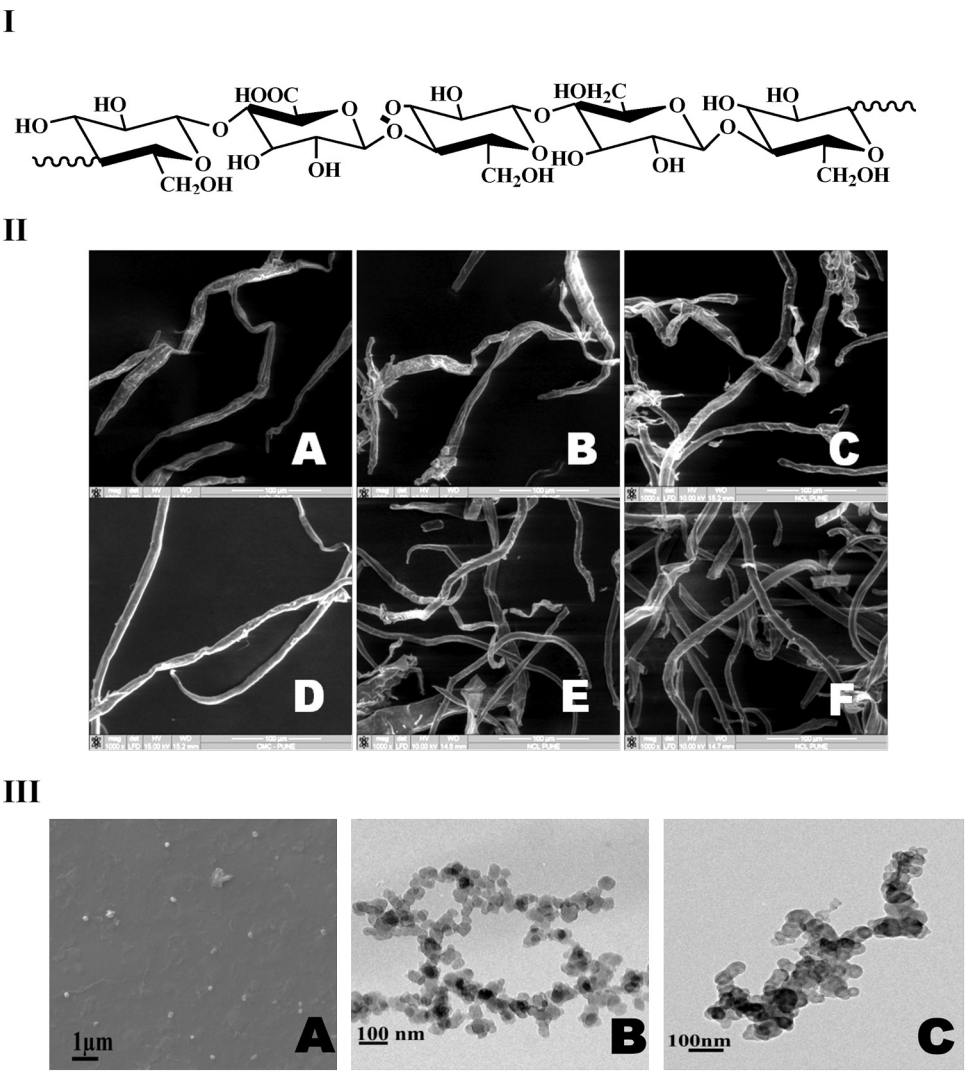

Fig. 1. (I) Structure of 6-carboxy cellulose (6CC); 1–22% carboxyl content. (II) SEM images (1000×) (100 μm) of non-nanosized fibrils of 6CC with varying carboxyl content (reaction performed for different time period at 25 °C): (A) cellulose, (B) 1 h (1.7%), (C) 3 h (3.0%), (D) 6 h (8.6%), (E) 12 h (14.0%), and (F) 24 h (19.7%). (III) (A) SEM of 6CC (nanoparticles) prepared at 50 °C (13.2%). (B) TEM of 6CC (nanoparticles) prepared at 50 °C (13.2%). (C) TEM of 6CC (nanoparticles) prepared at 40 °C/48 h (21.5%).

25% yield (16% carboxyl) was obtained at 40 °C/24 h reaction time at as compared to 63% yield (19.7% carboxyl) for the 25 °C/24 h reaction. A major change was observed beyond the 24 h reaction at 40 °C: now nanoparticles started to be observed, but with a yield of only 5% (Table 1). This encouraged us to attempt higher temperatures and lower reaction times, so as to maximize the nanoparticles yield. Indeed, we observed that at 50 °C/12 h, we obtained only nanoparticles, with a yield of 46%. Going higher, at 70 °C/8 h, we again obtained only nanoparticles, but with a reduced yield of 16%. This shows that a temperature range around 50 °C and low reaction times of upto 12 h is needed to maximize nanoparticle yields. In order to obtain only macro-sized fibrils and no nanoparticles, the lower reaction temperature of 25 °C is favorable. The morphologies were confirmed by SEM and TEM studies, and representative pictures are shown in Fig. 1(II-A and B). Fig. 1(II-C) shows the SEM of the macro-sized fibrils obtained at 25–40 °C at low reaction times. It is clearly seen that the sizes of the nanoparticles are between 25 and 35 nm, and they are quasi-spherical in shape Fig. 1(II-B). This is in contrast to the TEMPO oxidation method, where only elongated nanofibrils were obtained (Isogai et al., 2011). A study of the molecular weights of the 6-carboxycellulose products showed that upto 50 °C, the degree of polymerization (DP) was in the range of 70–87 (lower DP at higher reaction times), followed by a significantly reduced DP of 50 at 70 °C. Thus, it was possible to control the molecular weights and yields of the 6-carboxycelluloses by controlling the reaction temperature and time. It may be mentioned, that lower molecular weights may be beneficial for cellular uptake studies, especially for bioimaging studies after attaching fluorescent probes.

TGA of the samples (Table 2 and Fig. 2) shows that even with very low degrees of carboxyl functionalization, 6-carboxycellulose exhibited significantly reduced thermal stability as compared to the original cellulose, and the onset of degradation temperature was a function of the degree of oxidation (i.e., carboxyl content). For the original cellulose, the maximum degradation occurs in the range of 320–377 °C and the TGA curve showed a single step degradation curve and maximum degradation in a narrow range (50% weight loss at 353 °C). Even for samples with a carboxyl content as low as 1.7%, the onset of degradation came down to 213 °C, and thereafter reduced incrementally for more extensive oxidations, finally reaching to 154 °C for 21.5% carboxyl content. When the reaction temperature was 25 °C, for the carboxyl content 22% (sample no. 8, Table 2) the T_{onset} was 178 °C, while at a reaction temperature of 40 °C for the same extent of carboxyl content, the T_{onset} was 154 °C (sample 14, Table 2). This was due to greater degradation of the molecular weight and reduced crystallinity of the product at the

Table 2
TGA data of 6CCs prepared at 25 °C, 40 °C, 50 °C and 70 °C.

Sr. No.	Sample name (time/temp.)	Oxidation (%)	T_{onset} (°C)	$T_{final\ deg.}$ (°C)	T_{50} (°C)	Residue (wt.%)
1	Cellulose[a]	0	320	377	353	5
2	Amorphous[b] cellulose	0	222	ND	326	26
25 °C						
3	1 h	1.7	213	ND	302	12
4	3 h	3.0	206	ND	293	15
5	6 h	8.6	204	ND	296	13
6	12 h	14.1	188	ND	282	12
7	24 h	19.7	184	ND	266	9
8	48 h	22.0	178	ND	247	6
40 °C						
9	1 h	6.17	213	ND	300	9
10	3 h	13.2	182	ND	288	11
11	6 h	14.3	177	ND	288	11
12	12 h	14.0	169	ND	262	15
13	24 h	16.0	166	ND	252	16
14	48 h	17.0 I crop	164	ND	251	16
	48 h	21.5 II crop; NP	154	ND	244	20
50 °C						
15	12 h	13.2 NP	172	ND	282	17
70 °C						
16	8 h	13.9 NP	146	ND	293	11

T_{onset} – onset degradation temperature.
$T_{final\ deg.}$ – final degradation temperature.
T_{50} – temperature at which 50% weight loss occurred.
Residue (wt.%) – weight remained at 850 °C.
ND – not determined.
NP – nano-particle.
[a] Sugarcane derived cellulose.
[b] Amorphous cellulose.

higher reaction temperature, keeping the reaction time constant (48 h). When the reaction temperature was further increased to 50 °C, the T_{onset} was 172 °C, even though the reaction was stopped after 12 h (sample 15, Table 2). The T_{50} (temperature for 50% wt. loss) also decreased in a similar fashion with increasing carboxyl content, reaching 244 °C for the 21.5% carboxyl content sample. At 70 °C reaction temperature where the 6-carboxycellulose undergoes more severe degradation reactions, the T_{onset} was further reduced to 146 °C. Comparison with literature results of thermal analysis of partially C6-carboxylated cellulose nanofibrils also confirmed that the thermal decomposition is severely affected by the glucuronic acid moiety due to decarbonation during the heating process. The onset of degradation for the cellulose nanofibril films was about 200 °C, comparable to the samples nos. 4–8 (upto 19% carboxyl content) in Table 2 (Fukuzumi, Saito, Iwata, Kumamoto, & Isogai, 2009; Fukuzumi, Saito, Okita, & Isogai, 2010). Further comparing the thermal stability of nanoparticles of 6-carboxycellulose with the macro-sized 6-carboxycelluloses of the same carboxyl content (samples 10 and 15 of Table 2 with 13.2% carboxyl content), we see that the nanoparticles had a T_{onset} of 172 °C while the non-nano particle had a T_{onset} of 182 °C. However, this decrease in T_{onset} for the nanoparticle is most likely due only to the higher reaction temperature of sample 15 causing greater degradation of the polymer molecule. Thus, from the TGA data it appears that nano and non-nano particles have similar thermal stabilities. It should be noted from the TGA curves that while pure cellulose showed

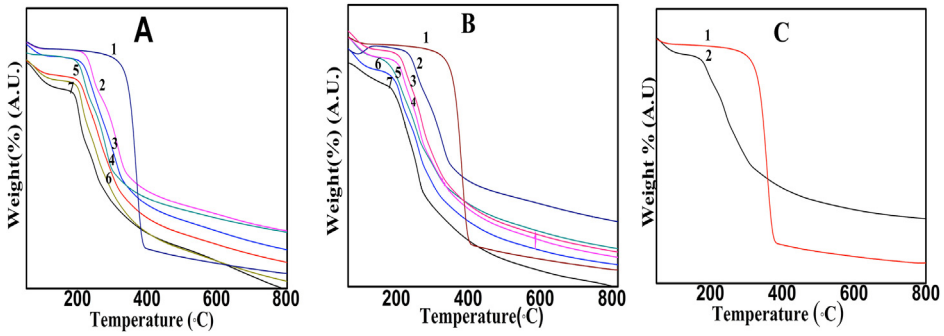

Fig. 2. TGA of cellulose and 6CC of various COOH contents (%). (A) Prepared at 25 °C: (1) cellulose, (2) 1.7%, (3) 3.0%, (4) 8.6%, (5) 14.1%, (6) 19.7%, and (7) 22.0%. (B) Prepared at 40 °C: (1) cellulose, (2) 6.17%, (3) 13.2%, (4) 14.3%, (5) 14.0%, (6) 16.0%, and (7) 17.0%. (C) TGA of (1) cellulose and (2) 6CC-nanoparticles prepared at 50 °C (13.2% COOH content).

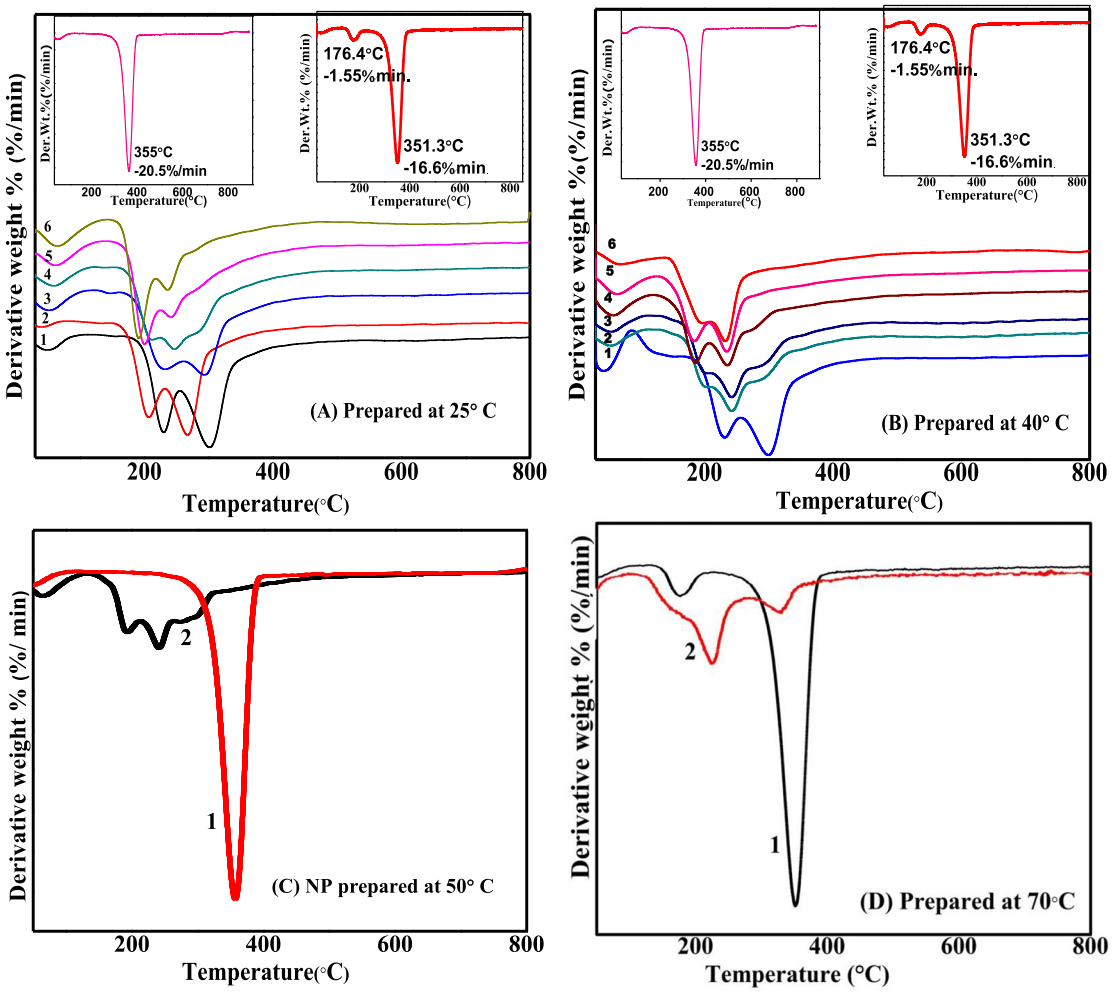

Fig. 3. DTG of 6CC of various COOH contents (%).
(A) Prepared at 25 °C: (1) 1.7%, (2) 3.0%, (3) 8.6%, (4) 14.1%, (5) 19.7%, and (6) 22.0%. (B) Prepared at 40 °C: (1) 6.17%, (2) 13.2%, (3) 14.3%, (4) 14.0%, (5) 16.0%, and (6) 17.0%, inset left: cellulose, inset right: physical mixture 20:80%, w/w, glucuronic acid:cellulose I (in both graphs (A) and (B)). (C) DTG of (1) cellulose and (2) 6CC-NP prepared at 50 °C (13.2%). (D) DTG of (1) cellulose and (2) 6CC-nanoparticles prepared at 70 °C (13.9%).

a single step degradation curve, their carboxy derivatives showed multi-step degradation curves. 6-Carboxycellulose can be considered to be a copolymer of glucose (G) and glucuronic acid (GA), with the latter decomposing at much lower temperature. As the carboxy content increases, the GA content of the 6-carboxycellulose increases, causing increased degradation at higher temperatures. These results indicated that presence of glucuronic acid was the major cause of thermal destabilization of cellulose, while molecular weight, and shape and size of the nanoparticle did not significantly affect thermal stability. This effect was seen more clearly in the differential thermogravimetry (DTG) curves, explained in the following paragraph.

The DTG curve measures the rate of weight loss with respect to temperature and shows accurately the point where weight loss is maximum. The DTG data for cellulose I, cellulose I + glucuronic acid, (80:20, w/w, approximately corresponding to the highest extent of carboxyl content in the 6-carboxycellulose samples), amorphous cellulose, and various 6-carboxycellulose samples is presented in Table 1S and Fig. 3. A single sharp DTG curve is observed for cellulose at 355 °C, while the cellulose + glucuronic acid (GA) mixed sample showed a sharp peak at 351 °C corresponding to cellulose and another sharp peak at 176 °C corresponding to the GA added to the cellulose. Looking at the data for the 6-carboxycellulose samples, it is clear that they fall in three categories: below 14% carboxyl content two well resolved peaks are observed, in which the major peak at higher temperature (291–302 °C) corresponds to the crystalline portion of cellulose I and the minor peak at lower temperature (around 228 °C) corresponded to the amorphous peak which we speculate included the glucuronic moiety. At around 14% carboxyl content (sample nos. 7, 11, 12, 13, 16, 17 in Table 1S) there was a clear transition to three peaks, the lowest temperature peak at 211 °C corresponds to the GA, the middle peak at 246 °C corresponds to the amorphous cellulose peak, and the highest temperature peak (286 °C) was the residual crystalline cellulose peak. The crystalline peak had shifted to a lower value due to the carboxyl functionalization and lower DP. Now, as we go to 16–21.5% carboxyl content (samples 7, 8, 15, 16, in Table 1S), a reverting back to two peaks was observed, as in samples with <8% carboxyl. Here the peak corresponding to the amorphous peak (merged with the glucuronic moiety) was the major peak (at lower temperature, 183 °C,) while the crystalline cellulose was the minor peak (at the higher temperature 233 °C). As the carboxyl content increased, all peaks shifted to lower values. These interpretations and transitions were more clearly seen in Fig. 4, where the DTG curves of selected samples of 6-carboxycellulose are overlaid with the control samples of cellulose, amorphous cellulose, and cellulose + GA. It was observed that with the progress of the carboxylation reaction, there were gradual changes in the morphological structure. Such a study of morphological changes occurring in a cellulosic polymer molecule with progressive oxidation, showing a continuous shift in the crystalline

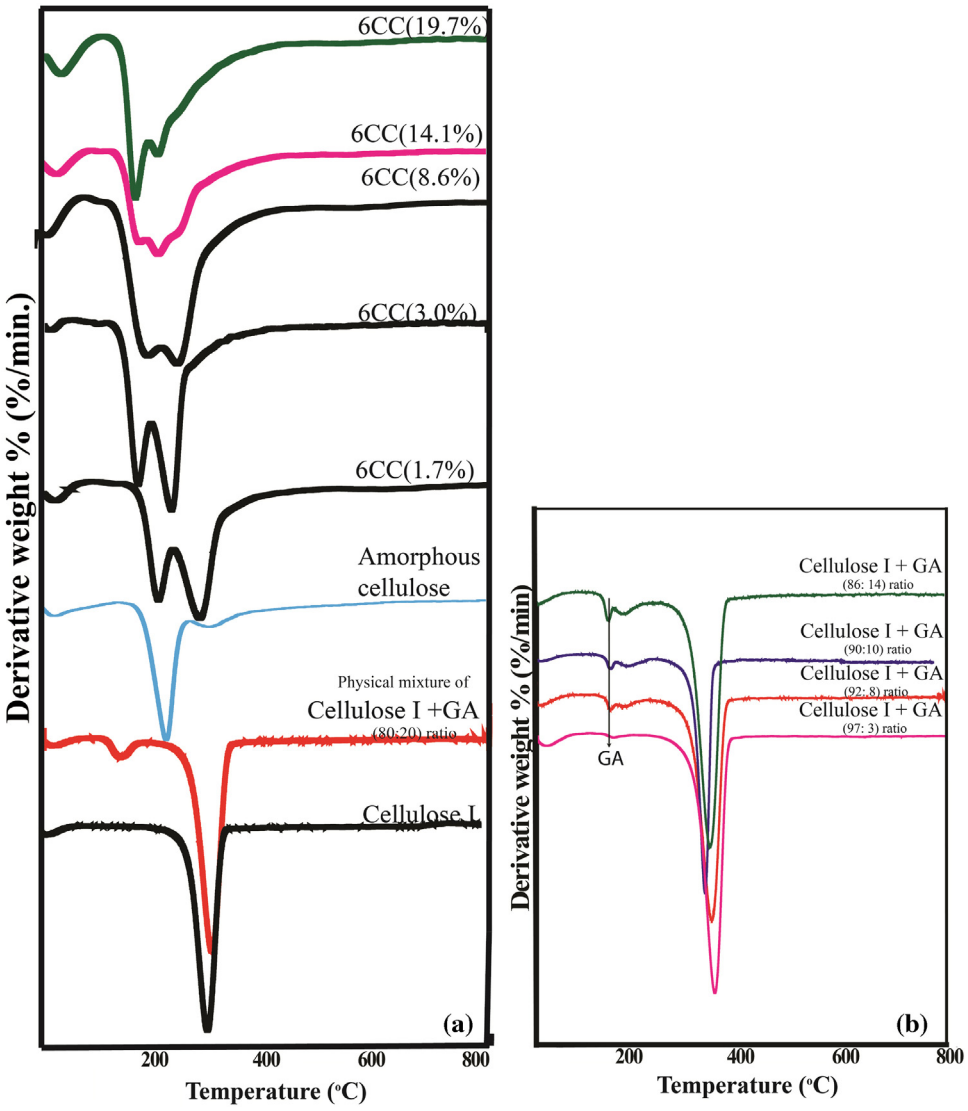

Fig. 4. (A) Overlay DTG curves of cellulose, cellulose I + GA (physical mixture 20:80 ratio), amorphous cellulose, 6CC (1.7%), 6CC (3.0%), 6CC (8.6%), 6CC (14.1%) and 6CC (19.7%). (B) Overlay DTG curves of cellulose I + GA – physical mixture in various ratios: (97:3), (92:8), (90:10), and (86:14).

peak to lower values with degree of oxidation, and the merging of the glucuronic peak under the amorphous peak below and above a critical point (~14% oxidation) has not been reported.

Another important property of these series of compounds is their solubililty. The solubility of oxidized 6-carboxycellulose was studied in different concentrations of alkali (NaOH) from 0.2% to 10% (Table 1B and C). The 6-carboxycellulose (22% carboxyl content) was easily soluble even at 0.2% alkali solution. Recent literature shows the solubility of 21.29% oxidized cellulose in 0.2 M NaOH (0.8%) (Wu, He, Huang, Wang, & Tang, 2012). The much lower concentration of alkali needed for dissolution in our case could be due to the lower molecular weight and higher amorphous content of our sample. Expectedly, as the carboxyl percent increased, the solubility of 6-carboxycellulose was found to continuously increase in alkali solution. The solubility was also studied in a variety of organic solvents. The 6-carboxycellulose (22% carboxyl) was partially soluble in DMSO; none of the other solvents showed solubility, though there appeared to be swelling in some solvents like pyridine and DMF. The solubility or swelling of oxidized celluloses in organic solvents can lead to their facile transformation by a variety of organic chemical reactions and result in several new products. Thus, 6CC can be used as a platform polymer to produce series of new molecules.

4. Conclusions

TGA/DTG studies of the new series of series of 6-carboxycellulose molecules were used to assess the thermal stability of low molecular weight spherical nanoparticles of 6CCs of different carboxyl contents, which have been synthesized and characterized for the first time. It was found that the thermal behavior of the nanoparticles of 6CC were similar to that of the non-nano sized analogs, implying that the particle size had no effect on the thermal stability. This is important for applications in biocomposites, where curing at higher temperatures maybe required. These studies also threw light on the morphological changes occurring with the changes in the carboxyl content (continuous shift in the crystalline peak to lower values with degree of oxidation, and the merging of the glucuronic peak under the amorphous peak below and above a critical point of 14% oxidation). The solubility data shows that 6-carboxycelluloses (22% carboxyl) is easily soluble in low concentration of (0.2%) alkali. This sample

also shows partial solubility in DMSO, and swells in some solvents like pyridine and DMF. These factors improve the versatility of the 6-carboxycelluloses and their nanoparticles for enabling further chemical modification through the carboxyl groups.

Acknowledgements

AJV thanks CSIR funding this research under the 12th. Five Year plan projects, and PRS thanks CSIR-HRDG for funding her Senior Research Fellowship for the doctoral degree research.

Appendix A. Supplementary data

Supplementary data associated with this article can be found, in the online version, at http://dx.doi.org/10.1016/j.carbpol.2014.01.015.

References

Anderson, H. E., & McIntyre, A. R. (1946). Successful use of oxidized cellulose in surgery of the uterus. *Science*, *104*, 301.
Arendt, J. H., Carriere, J. P., Bouchez, P., & Sachetto, J. P. (1973). Oxidation of cellulose by acid–sodium nitrite systems. *Journal of Polymer Science*, 1521–1529 (Symposium No. 42)
Cheng, G., Varanasi, P., Li, C., Liu, H., Melnichenko, Y. B., Simmons, B. A., et al. (2011). Transition of cellulose crystalline structure and surface morphology of biomass as a function of ionic liquid pretreatment and its relation to enzymatic hydrolysis. *Biomacromolecules*, *12*(4), 933–941.
Coseri, S., Biliuta, G., Simionescu, B. C., Kleinschek, K. S., Ribitsch, V., & Harabagiu, V. (2013). Oxidized cellulose – Survey of the most recent achievements. *Carbohydrate Polymers*, *93*, 207–215.
Crawford, R. J., Edler, K. J., Lindhoud, S., Scott, J. L., Janet, L., & Unali, G. (2012). Formation of shear thinning gels from partially oxidised cellulose nanofibrils. *Green Chemistry*, *14*, 300–302.
Cross, C. F., & Bevau, E. J. (1883). On the oxidation of cellulose. *Journal of Cell Science*, *43*, 22.
Eichhorn, S. J. (2011). Cellulose nanowhiskers: Promising materials for advanced applications. *Soft Matter*, *7*, 303.
Fink, H. P., Weigel, P., Purz, H. J., & Ganster, J. (2001). Structure formation of regenerated cellulose materials from NMMO-solutions. *Progress in Polymer Science*, *26*, 1473–1524.
Fukuzumi, H., Saito, T., Okita, Y., & Isogai, A. (2010). Thermal stabilization of TEMPO-oxidized cellulose. *Polymer Degradation and Stability*, *95*, 1502–1508.
Fukuzumi, H., Saito, T., Iwata, T., Kumamoto, Y., & Isogai, A. (2009). Transparent and high gas barrier films of cellulose nanofibers prepared by TEMPO-mediated oxidation. *Biomacromolecules*, *10*, 162–165.
Houser, K. M. (1946). Oxidized cellulose gauge packing for nasal bleeding. *JAMA: The Journal of the American Medical*, *132*, 143.
Isogai, A., Saito, T., & Fukuzumi, H. (2011). TEMPO-oxidized cellulose nanofibers. *Nanoscale*, *3*, 71–85.
Isogai, A., & Kato, Y. (1998). Preparation of polyuronic acid from cellulose by TEMPO-mediated oxidation. *Cellulose*, *4*, 153–164.
Kennedy, H. P. (1947). Familial hemorrhagic telangiectasia – With a note on the use of oxidized cellulose gauze as a hemostatic agent in epistaxis. *The New England Journal of Medicine*, *237*(6), 180.
Klemm, D., Heublin, B., Fink, H., & Bohn, A. (2005). Cellulose: Fascinating biopolymer and sustainable raw material. *Angewandte Chemie International Edition*, *44*, 3358–3393.
Klemm, D., Kramer, F., Moritz, S., Lindstrom, T., Ankerfors, M., Gray, D., et al. (2011). Nanocelluloses: A new family of nature-based materials. *Angewandte Chemie International Edition*, *50*, 5438–5466.
Kulterer, M. R., Reichel, V. E., Kargl, R., Kostler, S., Sarbova, V., Heinze, T., et al. (2012). Functional polysaccharide composite nanoparticles from cellulose acetate and potential applications. *Advanced Functional Materials*, *22*, 1749.
Kumar, V., & Yang, T. (2002). HNO_3/H_3PO_4–$NaNO_2$ mediated oxidation of cellulose – Preparation and characterization of bioabsorbable oxidized celluloses in high yields and with different levels of oxidation. *Carbohydrate Polymers*, *48*, 403–412.
Lin, N., Huang, J., & Dufresne, A. (2012). Preparation, properties and applications of polysaccharide nanocrystals in advanced functional materials: A review. *Nanoscale*, *4*, 3274–3294.
Nachtkamp, K., Kruger, C., Engelhardt, J., Kriegisch, V., Fischer, S., & Pinnow M., et al. (2012). *Nanoparticles from slightly oxidised cellulose*. US Patent 8,338,494.
Nikolajaski, M., Wotschadlo, J., Clement, J. H., & Heinze, T. (2012). Amino-functionalized cellulose nanoparticles: Preparation, characterization, and interactions with living cells. *Macromolecular Bioscience*, *12*, 920.
Nooy, A. E. J., Pagliaro, M., Bekkum, H. V., & Besemer, A. C. (1997). Autocatalytic oxidation of primary hydroxyl functions in glucans with nitrogen oxides. *Carbohydrate Research*, *304*, 117.
Nuruddin, M., Chowdhury, A., Haque, S. A., Rahman, M., Farhad, S. F., Sarwar Jahan, M., et al. (2011). Extraction and characterization of cellulose microfibrils from agricultural wastes in an integrated biorefinery initiative. *Cellulose Chemistry and Technology*, *45*(5–6), 347–354.
Okita, Y., Saito, T., & Isogai, A. (2010). Entire surface oxidation of various cellulose microfibrils by TEMPO-mediated oxidation. *Biomacromolecules*, *11*, 1696–1700.
Sasaki, M., Adschiri, T., & Arai, K. (2003). Production of cellulose II from native cellulose by near- and supercritical water solubilization. *Journal of Agricultural and Food Chemistry*, *51*, 5376–5381.
Scarff, J. E., Stookey, B., & Garcia, F. (1949). The use of dry oxidized cellulose as a primary hemostatic agent in neurosurgery. *Journal of Neurosurgery*, *6*, 304.
Sharma, P. R., & Varma, A. J. (2013). Functional nanoparticles from cellulose: Engineering the shape and size of 6-carboxycellulose. *Chemical Communications*, *49*, 8818–8820.
Shi, Z., Philpis, G. O., & Yang, G. (2013). Nanocellulose electroconductive composites. *Nanoscale*, *5*, 3194–3201.
Shinoda, R., Saito, T., Okita, Y., & Isogai, A. (2012). Relationship between length and degree of polymerization of TEMPO-oxidized cellulose nanofibrils. *Biomacromolecules*, *13*, 842–849.
Stamm, A. J. (1964). *Wood and cellulose science*. NY: Ronald Press Co.
USP. (1995). *United States Pharmacopeia 23/National Formulary 18. Oxidised cellulose*.
Varma, A. J. (2013). *A process for fractionating sugarcane bagasse into high alpha-cellulose pulp, xylan and lignin*. China Patent ZL 200880111416.3.
Varma, A. J., & Sharma, P. R. (2013). *Antimicrobial activity of nano-sized carboxycellulose*. Indian Patent 2758DEL2013.
Varma, A. J., & Chavan, V. B. (1994). Cellulosic diamines as reaction-incorporated filler in epoxy composites. *Cellulose*, *1*, 215–219.
Wei, S., Kumar, V., & Banker, G. S. (1996). Phosphoric acid mediated depolymerization and decrystallization of cellulose: Preparation of low crystallinity cellulose – A new pharmaceutical excipient. *International Journal of Pharmaceutics*, *142*, 175–181.
Wu, Y. D., He, J. M., Huang, Y. D., Wang, F. W., & Tang, F. (2012). Oxidation of regenerated cellulose with nitrogen dioxide/carbon tetrachloride. *Fibers and Polymers*, *13*, 576–581.
Yackel, E. C., & Kenyon, W. O. (1942). The oxidation of cellulose by nitrogen dioxide. *Journal of the American Chemical Society*, *64*, 121.
Zhou, Y., Fuentes-Hernandez, C., Khan, T. M., Liu, J., Hsu, J., Shim, J. W., et al. (2013). Recyclable organic solar cells on cellulose nanocrystal substrates. *Scientific Reports*, *3* (Article No. 1536).
Zimnitski, D. S., Yurkshtovich, T. L., & Bychkovsky, P. M. (2004). Synthesis and characterization of oxidized cellulose. *Journal of Polymer Science, Part A: Polymer Chemistry*, *42*, 4785–4791.